2002-01-3300 Design, Analysis and Testing of a Formula SAE Car Chassis

Article · December 2002

DOI: 10.4271/2002-01-3300

2 authors, including:

Albert George
Cornell University
93 PUBLICATIONS **1,142** CITATIONS

SEE PROFILE

SAE TECHNICAL PAPER SERIES

2002-01-3300

Design, Analysis and Testing of a Formula SAE Car Chassis

William B. Riley and Albert R. George
Cornell University

Reprinted From: Proceedings of the 2002 SAE Motorsports Engineering Conference and Exhibition (P-382)

Motorsports Engineering Conference & Exhibition
Indianapolis, Indiana
December 2-5, 2002

ISSN 0148-7191

Printed in USA

2002-01-3300

Design, Analysis and Testing of a Formula SAE Car Chassis

William B. Riley[1] and Albert R. George
Cornell University

ABSTRACT

This paper is taken from work completed by the first author as a member of the 1999 Cornell University Formula SAE Team and discusses several of the concepts and methods of frame design, with an emphasis on their applicability to FSAE cars. The paper introduces several of the key concepts of frame design both analytical and experimental. The different loading conditions and requirements of the vehicle frame are first discussed focusing on road inputs and load paths within the structure. Next a simple spring model is developed to determine targets for frame and overall chassis stiffness. This model examines the frame and overall chassis torsional stiffness relative to the suspension spring and anti-roll bar rates. A finite element model is next developed to enable the analysis of different frame concepts. Some modeling guidelines are presented for both frames in isolation as well as the assembled vehicle including suspension. Finally, different experimental techniques are presented to determine what stiffness is actually achieved from a constructed vehicle. A comparison of frames tested in isolation versus whole vehicle testing is made, and a simple whole-car chassis torsion test method is discussed.

INTRODUCTION

This paper examines several aspects of vehicular frame design, with an emphasis on application to an open-wheeled, space-frame racecar chassis, as is used in Formula SAE (FSAE). The FSAE competition is sponsored by the Society of Automotive Engineers (SAE).

Some key questions that have been raised from year to year in designing FSAE cars at Cornell University are: What is the best way to transfer the loads through the structure? What are the deformation modes of the structure? How stiff should the frame be in each of the deformation modes? How does the frame stiffness affect the dynamic response of the car? All of these questions are discussed to varying degrees in this paper.

VEHICLE LOADING

The first step to designing a vehicle frame, or any structure, is to understand the different loads acting on the structure. The main deformation modes for an automotive chassis are given in [8] as:

1. Longitudinal Torsion
2. Vertical Bending
3. Lateral Bending
4. Horizontal Lozenging

1. Longitudinal Torsion

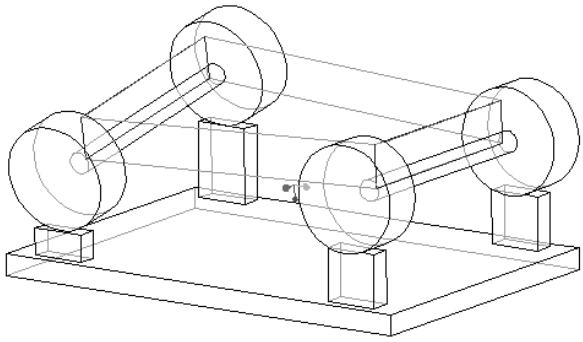

Figure 1: Longitudinal Torsion Deformation Mode

Torsion loads result from applied loads acting on one or two oppositely opposed corners of the car. The frame can be thought of as a torsion spring connecting the two ends where the suspension loads act. Torsional loading and the accompanying deformation of the frame and suspension parts can affect the handling and performance of the car. The resistance to torsional deformation is often quoted as stiffness in foot-pounds per degree. This is generally thought to be the primary determinant of frame performance for a FSAE racecar.

[1] Currently with Ford Motor Company

2. Vertical Bending

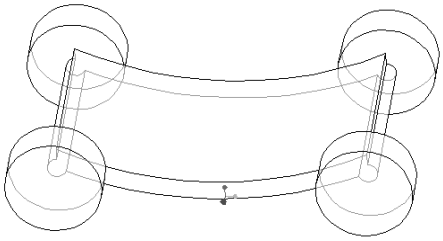

Figure 2: Vertical Bending Deformation Mode

The weight of the driver and components mounted to the frame, such as the engine and other parts, are carried in bending through the car frame. The reactions are taken up at the axles. Vertical accelerations can raise or lower the magnitude of these forces.

3. Lateral Bending

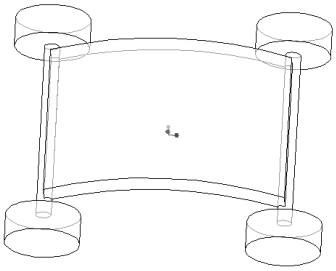

Figure 3: Lateral Bending Deformation Mode

Lateral bending loads are induced in the frame for various reasons, such as road camber, side wind loads and centrifugal forces caused by cornering. The side-ways forces will act along the length of the car and will be resisted at the tires. This causes a lateral load and resultant bending.

4. Horizontal Lozenging

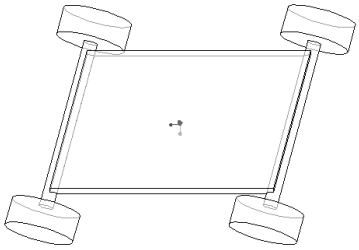

Figure 4: Horizontal Lozenging Deformation Mode

Forward and backward forces applied at opposite wheels cause this deformation. These forces may be caused by vertical variations in the pavement or the reaction from the road driving the car forward. These forces tend to distort the frame into a parallelogram shape as shown in the figure.

It is generally thought that if torsional and vertical bending stiffness are satisfactory then the structure will generally be satisfactory. Torsional stiffness is generally the most important as the total cornering traction is a function of lateral weight transfer.

STRAIN GAUGE DATA

The magnitude of the loads mentioned in the proceeding section changes with the operating mode of the car. Based on over ten years of experience with Cornell FSAE cars, parts designed to withstand both individual and combined 3.5 g bump, 1.5 g braking and 1.5 g lateral acceleration have been found to meet durability requirements. Thus, these loads have to be considered individually and together.

To verify these historical guidelines the 1998 Cornell Car was instrumented with strain gauges on the major suspension links. The strain gauge data was recorded at 100 Hz while the car was driven through several different representative tracks and situations. Some data from a skid pad run is shown below.

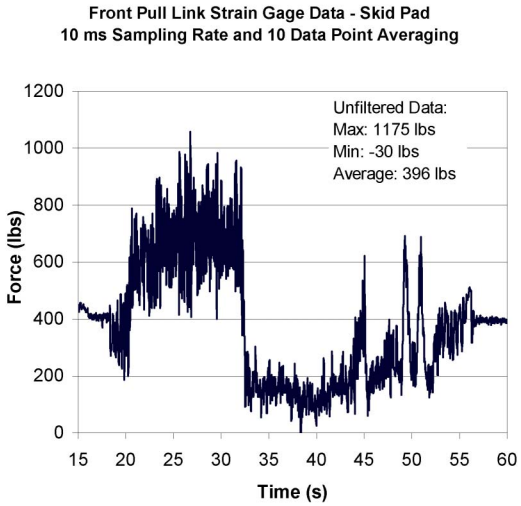

Figure 5: Strain Gauge Data

In one particular run the peak vertical force encountered on the corner of the car was 450 pounds, which corresponded to a vertical acceleration of 3.6 g's, assuming a 125 pound corner weight. This results in a stress of 19 KSI in a 0.5 in diameter pull link with a 0.028 in wall thickness.

The strain gauge data can also be used to gain insight in to the natural frequencies of the vehicle. This is accomplished by transforming the data from the time domain to the frequency domain and plotting the response. Taking one of the data files a fast Fourier transform was performed on the entire time history. Then plotting the coefficients versus the appropriate frequency we can observe spikes at the natural frequency of the system. For the first sample plot, we note a high-response at low frequencies, say below 2 Hz. There is another significant spike at roughly 5 Hz

and periodic spikes occurring at 8, 11, 15 Hz and so on. If we compare this data to an ANSYS natural frequency response prediction (albeit for a different car – the 1999 car), presented later, we observe the behavior is very similar. The peak at 5 Hz is not present on the ANSYS frequency response prediction. This suggests there may be something not accounted for in the ANSYS analysis, since the mass distribution and stiffness between the two cars is fundamentally the same.

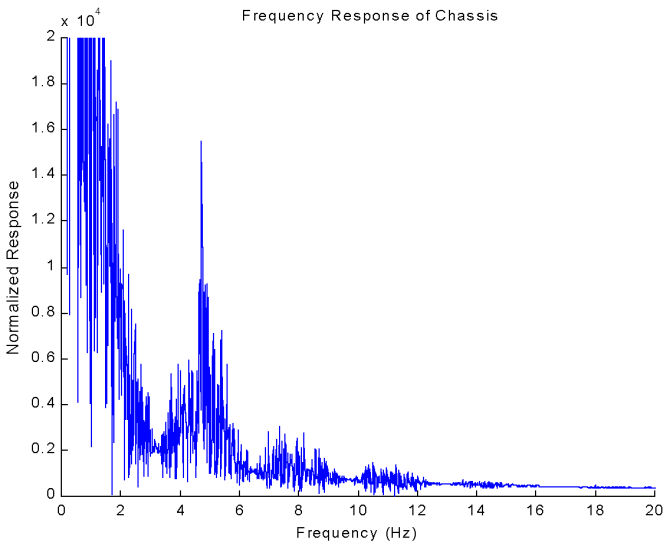

Figure 6: Strain Gauge Data

One possible source for the 5 Hz spike is the input from the rotationally unbalanced wheels. The strain gauge data was collected while the car drove around the skid pad. To check to see if the 5 Hz frequency is approximately correct, we can calculate roughly what the wheel frequency would have been on the skid pad. The calculation is simply the velocity of the car divided by the circumference of the wheel. Using an estimated car velocities in the test we get a frequency range of between 4-9 Hz. This shows that the peak around 5 Hz could easily be the rotary unbalance force.

We can also check to see above what frequencies the finite tire contact patch begins filtering out load inputs. Using the contact patch size we can find that frequencies over roughly 8 Hz should be filtered out for a quickly moving car. This doesn't account for engine or driver excited resonance at higher frequencies, simply the forcing done by the road on the car.

So, we see that generally, the 5 Hz spike can be accounted for by the unbalanced wheels. To check this hypotheis, a portion of the data was analyzed using the FFT and following the same procedure as outlined above. In this case, only the first few seconds were analyzed. During this time the car was mostly at rest or moving at only low speed. For this test we saw that the 5 Hz spike was missing, though the data was otherwise very similar to before. The magnitude of the responses were reduced, which makes sense given the lower force inputs in the second case. Presumably better balancing of the rotating components could reduce the exciting forces acting at this frequency.

CHASSIS STIFFNESS TARGETS

With the loading conditions discussed above it should now be possible to design the frame to be strong enough not to fail under the global loads acting on it for the different load cases. Just as importantly, however, is the stiffness of the entire chassis structure that affects the proper vehicle dynamics and handling. How stiff to make the structure is extremely difficult to determine empirically, and has to instead be based on experience gathered mostly from driver feedback. One way to approach the problem analytically is to examine how much of the overall vehicle compliance occurs in the structure compared to the deflections in the spring and tire. Obviously for an infinitely rigid chassis the car will respond only to the spring, damper and anti-roll bar changes. Some stiffness approaching the infinite case, then, should provide a stable platform for the suspension to do its job. A simple math model to examine this problem is to model the vehicle encountering a one wheel bump.

DEVELOPMENT OF ONE WHEEL BUMP MODEL

To look at the relative contributions of the spring, tire, suspension structure and frame structure we construct a series spring model of the vehicle encountering a one wheel bump. For beginning the model it is necessary to determine how to combine the effects of both linear springs (suspension springs) and torsion springs (frame and other chassis contributions).

To begin developing the model consider two tubes or other torsional members welded together, cantilevered from a wall, and loaded in torsion as shown below.

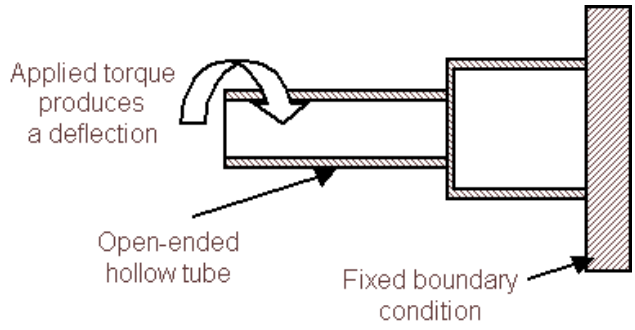

Figure 7: Tubes in Series

Here the tubes are shown in series. The deflection that occurs at the end of the assembly has a component from each of the two tubes. The stiffness, then, is also a function of the stiffness of each tube. If we use d to represent the flexibility of each tube then the flexibility of the system is just

$$d_{total} = d_1 + d_2$$

The stiffness is the inverse of the flexibility, which for the entire two-tube system can be found from

$$\frac{1}{K_{total}} = \frac{1}{K_1} + \frac{1}{K_2}$$

Which is the generic equation of stiffness for springs in series. If we had additional springs they would simply be taken into account by another term at the end of the equation. Another useful expression to model suspension effects will be to find the equivalent torsional stiffness for a linear spring at the end of a bar. A diagram is shown below.

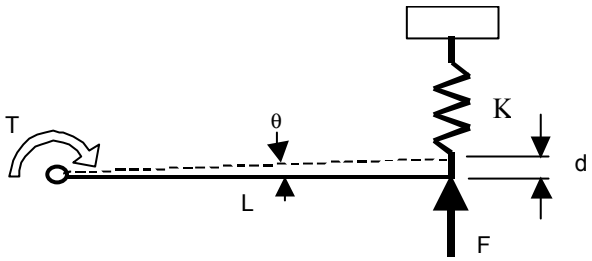

Figure 8: Linear to Torsion Spring

The diagram depicts a bar, pinned at one end, and connected to a linear spring at the other. The spring is fixed to ground at one end. From this information we wish to find the equivalent torsional spring constant for the system. For this calculation we need to find the torque the linear force is producing about the joint, and the angle the bar is moved through. While the diagram shows the force, F, and the displacement, d, we in fact know the spring constant, K_L. Knowing either K_L or F and d the other quantities can be calculated.

If we express K_T, the torsional spring stiffness, in units of in-lbs/radian then the equivalent linear spring stiffness, expressed in lbs/in and approximated using the small angle approximation is:

$$K_T \cong L^2 \cdot K_L$$

It is also possible to convert from torsional to linear spring stiffness in a similar manner. Performing the analysis we would find the general equation is

$$K_L \cong \frac{K_T}{L^2}$$

Now that we can model both torsion and linear springs in the same system, it is possible to build a model of all the compliant members in an automotive chassis. Depending on the desired complexity, different elements can be included or ignored in the model. The simplest model we will consider is to calculate the chassis stiffness for a rigid frame and compliant springs. In this model we assume the frame and suspension members are all infinitely stiff, and only the actual suspension springs themselves allow for any deflection. A picture of this model is shown below.

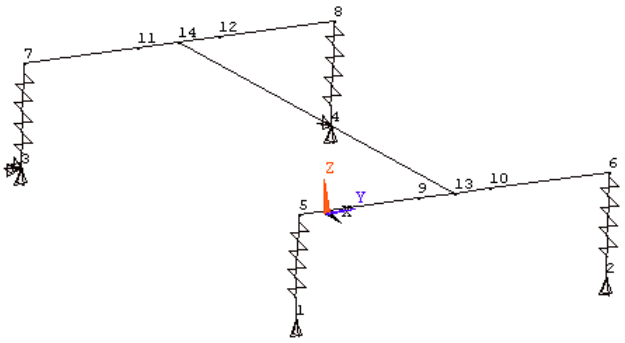

Figure 9: Vehicle Stick Model – Compliant Springs

The load is applied at the front left wheel (positive x and y direction). The other wheels are all constrained from motion in the vertical direction. We are neglecting forces and movement other than in the vertical direction, though the actual constraints are shown above. If we draw a free-body diagram of the model and solve using the sum of forces and moments we can determine that the changes in forces at all four wheels are equal. The back right wheel force is of the same direction as the applied load, while the other two wheels have their forces acting in the opposite direction, or trying to hold the car down. If we apply a force greater than the weight on those two wheels we would lift our car frame off the ground. For the purposes of this example, and in real world testing, we can assume that we have added weight to those corners to limit wheel lift. (The forces and deflections we are considering are all differences from the pre-existing forces/deflections that result from the car supporting its own weight.)

Since the force applied at each wheel is equal, call it F, the deflection of the spring at that wheel can be calculated if we know the spring constant, by the simple expression F=Kx. If we assume that each spring has the same rate, then the deflection of each spring will be equal. (If the springs have different rates, front/rear or even side-to-side, the method will still yield accurate results, but the relative motion of the nodes will change) Note in the figure the node numbers given. We constrained vertically three nodes, 1, 3 and 4. The four springs representing the suspension at the four corners of the car are all acting in series to resist the motion of the left wheel, or node 2. Therefore, the total response of the wheel, reacting against some applied load can be found by the following expression:

$$\frac{1}{K_{total}} = \frac{1}{K_1} + \frac{1}{K_2} + \frac{1}{K_3} + \frac{1}{K_4}$$

Here the subscripts simply denote each of the four springs.

The next model to consider is to represent the torsional compliance of the frame alone, a diagram of which is shown below.

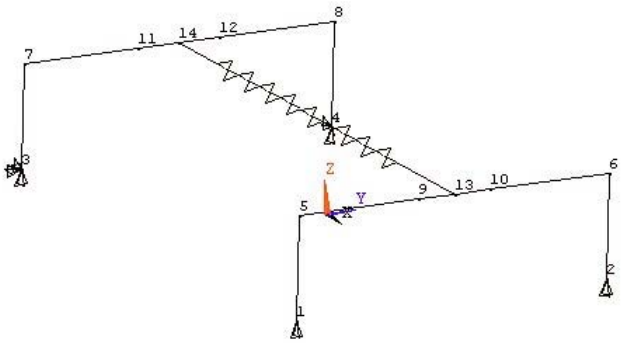

Figure 10: Vehicle Stick Model – Compliant Frame

In the above model a force applied at node 2, the contact patch, causes a torsional deflection in the frame. Since the other suspension elements are fixed, no other deflections occur. All other nodes remain at their initial position. Node 6 moves through a vertical deflection corresponding to the equivalent linear rate of the frame torsion spring. If the frame stiffness measured in ft-lbs/degree is equivalent to 100 lbs/in, then from a 100lb load node 2 deflects 1". It should be noted that the angle of the bar connecting nodes 5 and 6 will change during this condition, but we are considering only vertical deflections at this time.

Now we can use the principal of superposition to show that considering deflections from both the translational suspension springs and the frame torsion spring produces a deflection that is the sum of deflections occurring in each element. The spring-model considering the suspension and frame springs is shown below.

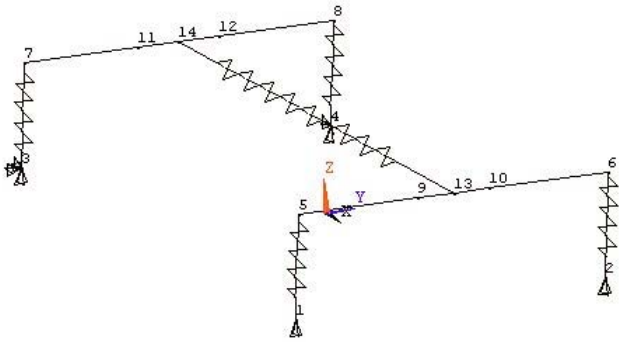

Figure 11: Vehicle Stick Model – Compliant Springs and Frame

The simple expression describing this behavior is as follows:

$$\frac{1}{K_{total}} = \frac{1}{K_1} + \frac{1}{K_2} + \frac{1}{K_3} + \frac{1}{K_4} + \frac{1}{K_5}$$

Note that K_5 is simply the spring constant of the torsion springs. In order to use this equation we must use consistent values of spring constants – either all translational spring values or all torsion spring values. We can convert back and forth by knowing the track and using the expression developed earlier in this section.

The suspension members, such as wishbones and rockers, also contribute compliance to the overall chassis system. This could be shown graphically as another torsion spring in series with the frame, and can be included in our whole-car stiffness equation. Also, note that we need to use the installed spring rate for each suspension spring. This installed spring rate will be the spring rate divided by the motion ratio squared. The squared term arises because the motion ratio affects both the force transmitted and the displacement the spring moves through. (Conservation of energy is one way to show the motion ratio must be squared.) A mathematical description of the complete system, using more description variable names is given below:

$$\frac{1}{K_{chassis}} = \frac{1}{K_{frame}} + \frac{1}{K_{suspension}} + \frac{r_1^{\,2}}{K_{spring\ 1}} + \ldots$$
$$\frac{r_2^{\,2}}{K_{spring\ 2}} + \frac{r_3^{\,2}}{K_{spring\ 3}} + \frac{r_4^{\,2}}{K_{spring\ 4}}$$

The variable r in the above expression is the motion ratio of the corresponding spring. Again, the units of spring stiffness must be consistently measured in equivalent stiffness for either a linear spring or rotary spring.

GRAPHICAL EXAMPLES

The model developed in the proceeding section allows the overall chassis stiffness to be calculated by knowing the spring rates of the frame, suspension structure and the actual installed suspension spring, or wheel rate. Selecting values of these elements for an actual design is one of compromise and tradeoff. To assist in this process example graphs are presented below to aid in the initial decision making process. To efficiently show these results and to make them general to any vehicle we can normalize all the stiffness values by the vehicle wheel rate. In this way the graphs can be used for any vehicle by simply expression the spring, suspension and frame stiffness as a ratio of the spring rate. Two graphs are shown below with these normalized values. The top graph presents the general case and the second graph captures the region that will usually be of interest in more detail. To use, simply cross reference the chassis stiffness by the suspension structure stiffness and read off the vehicle stiffness. These charts are constructed by graphing two springs acting in series. The final point on the graph for each series represents a rigid frame, so the magnitude of the vehicle stiffness will always equal the suspension stiffness. Additionally the case of rigid suspension is shown which means the resulting vehicle stiffness is equal to the chassis stiffness. The data series labeled "equal" represents equal suspension and chassis stiffness, which is convenient for maximizing the structural efficiency of the chassis/suspension system assuming relatively equal stiffness/weight ratios for both components.

Figure 12: Normalized Chassis Stiffness for Frame and Suspension Stiffness
Wheel Rate = "1"

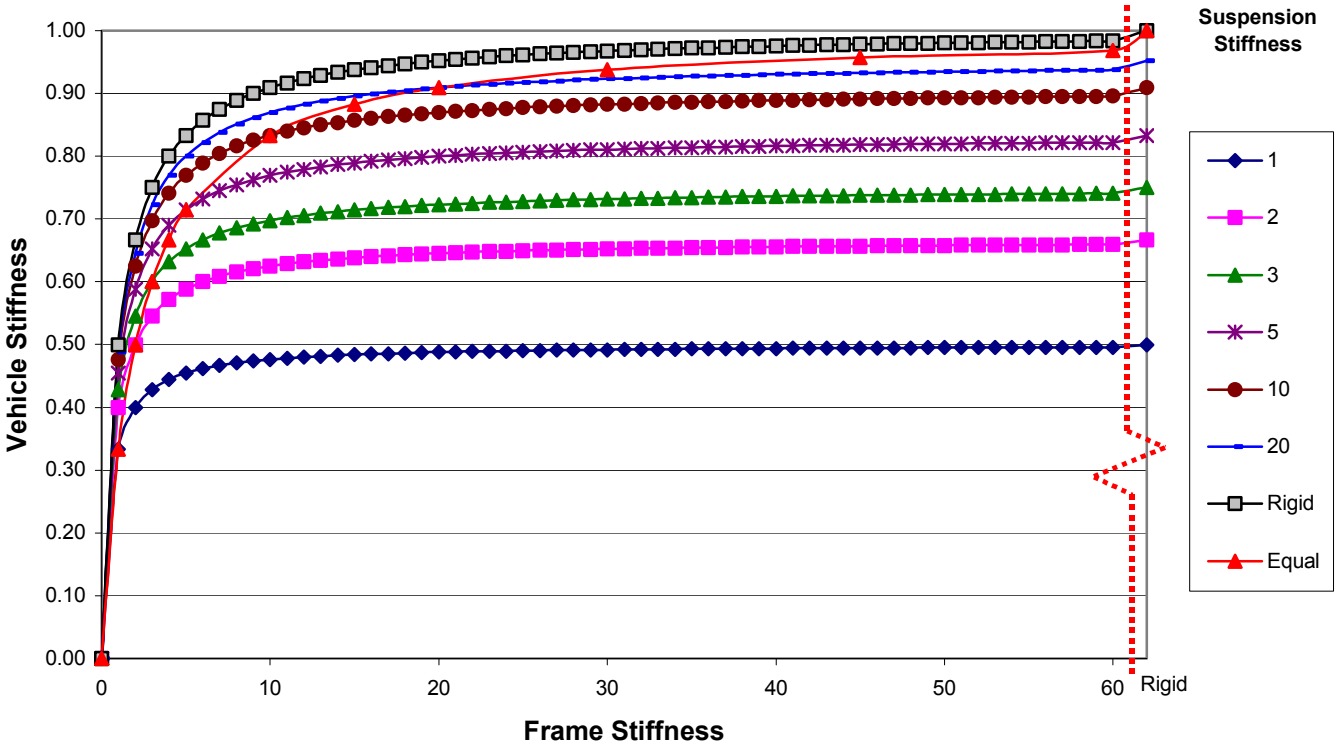

Figure 13: Normalized Chassis Stiffness for Varying Frame and Suspension Stiffness
Wheel Rate = "1"

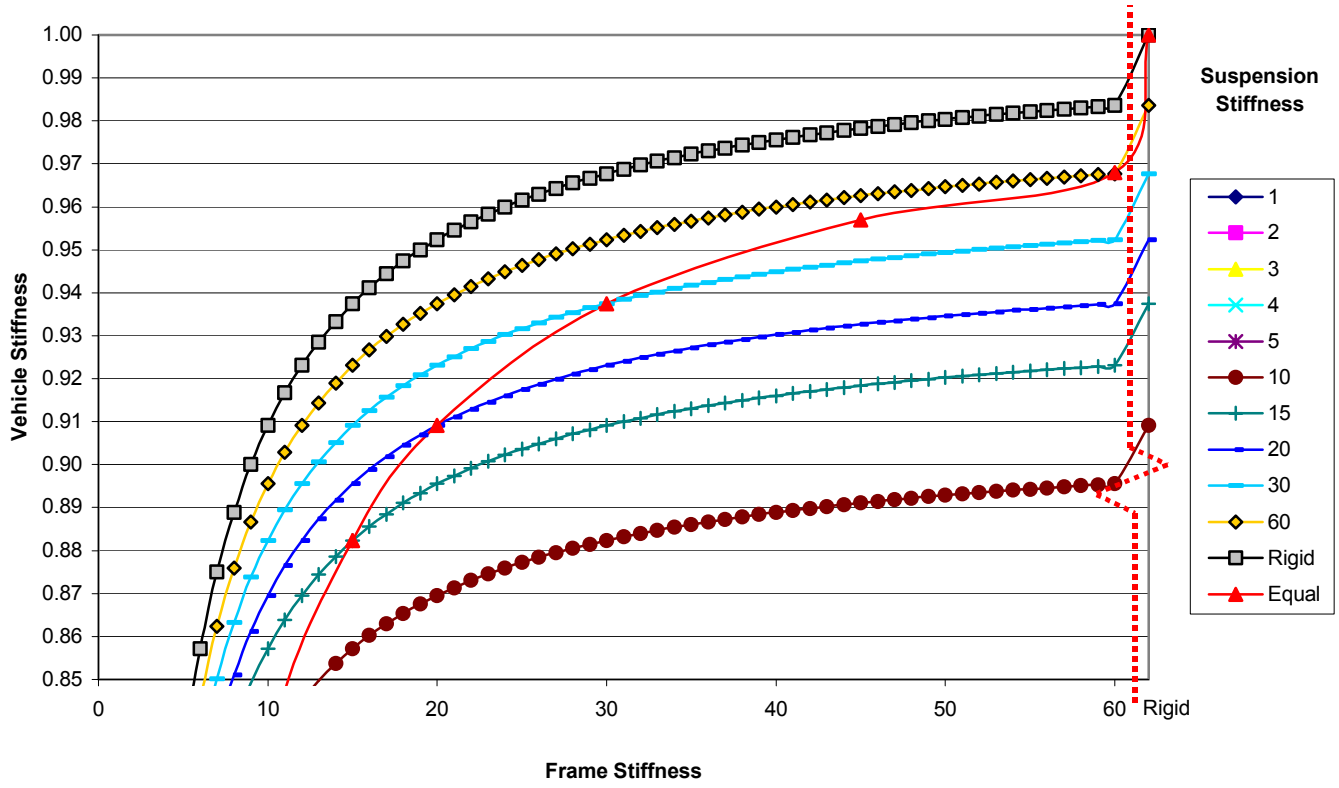

As an example of using the graph, say we desire a total vehicle stiffness that is 90% of the rigid case. For a chassis that is 10 times the wheel rate the suspension structural stiffness has to be roughly 60 times the wheel rate. For a chassis stiffness 20 times the wheel rate the suspension has to be roughly 17 times as stiff as the wheel rate. The charts are primarily useful for visualizing the trends of vehicle stiffness relative to the frame and suspension. For example if we know the suspension stiffness is 30 times the wheel rate than the graphs show that increasing the frame stiffness from 30 to 40 times the wheel rate only increases the vehicle stiffness by 0.5%. In most cases the designer will choose the reduced weight rather than that small an increase in stiffness.

FINITE ELEMENT MODEL DEVELOPMENT

FRAME AND WHOLE CHASSIS MODELING

To begin our explanation, a solid model of the 1999 car frame, drawn in Pro/Engineer with engine and wheels for reference, is pictured

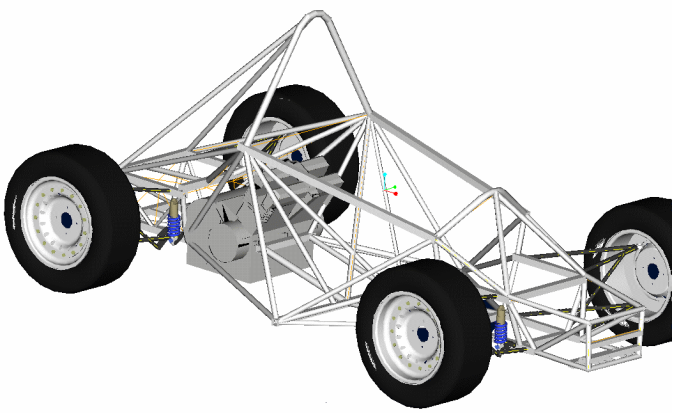

Figure 14: Vehicle Solid Model

The bare structural frame looks like the following:

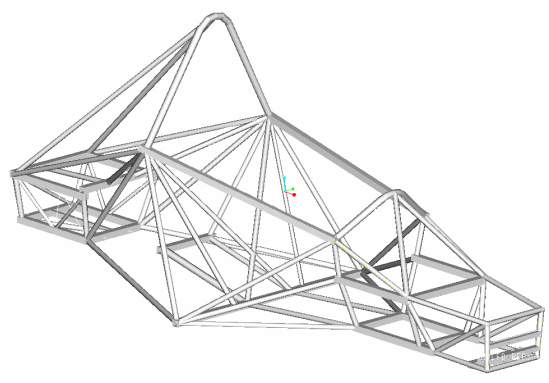

Figure 15: Frame Solid Model

To determine the stiffness of a proposed frame and chassis design before construction, a finite element model can be constructed to calculate the structures stiffness and strength. While the process of solving Finite Element problems is a science, creating the models is quite an art. There are many types of elements possible for representing a structure and every choice the analyst makes can affect the results. The number, orientation and size of elements as well as loads and boundary conditions are all critical to obtaining meaningful values of chassis stiffness.

Conventionally, the frame is decomposed into nodes and elements, with one element representing each tube on the car. Nodes are placed wherever more tubes join. Beam elements are normally used to represent each tube. The assumption made in using beam elements is that the welded tubes have stiffness in bending and torsion. If a truss or link element were used, the assumption being made would be the connections do not offer substantial resistance to bending or torsion. By examining various FSAE frames, we can see that while they are usually reasonably well triangulated, if some bending was not being resisted, some parts of many frames would become mechanisms and deflect substantially. Using beam elements to represent the frame itself has given good results for Cornell FSAE cars in the last few years. One other aspect of beam elements is the possibility of including transverse shearing effects. ANSYS automatically takes into account transverse shear, if the appropriate variables are included in the element definitions.

Another thing to consider when modeling just the frame is how to represent the engine and stressed skins. For the engine, the first step is to locate a node at each position where there is an engine mount. These mounts then need to be connected to the frame by an element representing the tab and engine mount. Previous testing has shown the engine to be very stiff relative to the car frame and can be mounted as a stressed component to reduce the frame weight. Testing has also shown that deflections experienced in the engine are much less than the bearing clearance and thus the engine is not damaged by carrying chassis torsional loads. This was true even for the 1993 Cornell car that was able to use the engine as the primary load carrying structure, because of the block design.

Thus, we can model the engine, assuming it to be infinitely rigid, by connecting each engine mount node to every other engine mount node by a beam element of high stiffness. In 1998 the engine tab element properties were modified until good agreement was reached between the experiments and the model. During the course of this project as the suspension was modeled the maximum number of elements was reached in the student version of ANSYS. One of the few things that could be done to reduce the number of elements was to replace the engine model just discussed with a solid block of aluminum, still connected to the frame by the engine tabs. This greatly reduced the complexity of the ANSYS model and produced

results that were practically unchanged compared to the other, multiple-tube engine model.

Stressed skins are much trickier to model than the engine. In real life, the stressed skins are composed of either 0.020" or 0.040" thick aluminum sheet bonded and riveted to the space frame. The simplest model is to connect a shear panel element from each of the four nodes on a side of the front suspension bay. Placing the stressed skins in the driver bay makes use of a combination of three and four sided elements. Using this method the analysis will usually predict a greater than measured value of stiffness due to the realities of the stressed skin installation which are not captured in the model. This difference will vary from frame to frame but from 20% to 50% of the predicted stiffness improvement (skins installed versus no skins) can be lost.

In addition to modeling the stiffness contribution from each part of the frame, we need to consider how to load and constrain the frame for an accurate analysis. By an accurate analysis we mean one that predicts the stiffness of the frame close to the actual stiffness as the frame operates in real world conditions. The problem here has normally been how to constrain and load a frame, as if it was receiving multiple load inputs from a suspension, while it has been separated from that suspension. In past years at Cornell, the back four nodes of the rear bay had been pinned or completely clamped depending on the year, and two equal and opposite forces had been applied at the front top of the front suspension bay. The problem with this boundary condition is that the optimal solution found from the FE analysis is to bring all triangulation to those pinned or clamped boundary nodes. In the actual car the rear of the car is supported at the tire/pavement interface, so the actual optimal design should tie to the several suspension pickup points rather than extreme edges of the frame.

To better understand the actual load paths and gauge the sensitivity of the design to boundary conditions it was decided to determine the torsional stiffness of the chassis for different loading assumptions. The first boundary condition tested was to clamp the front of the rear suspension bay, and see what affect that had on the stiffness of the frame. This increased the overall frame stiffness by several hundred foot-pounds per degree. The reason was that the entire rear bay of the car was virtually unloaded and barely deflecting. The discrepancy in the results raised the question of which model is more accurate? We knew that the model agreed closely with the experiments, but that did not tell us anything about if the experiments were representing the actual loading of the frame. It quickly became obvious the best way to settle the question was to model the entire suspension. This way, the loads could be put in as vertical wheel loads, and the other wheels could be constrained in such as a way that the whole structure was minimally constrained. Once the need to model the suspension was decided upon, research began on the best way to model the various suspension components. The a-arms, pull-links and several other components transmit tensile and compressive forces but no bending. These are modeled in ANSYS as link members. The uprights and connecting tabs are beams just like frame tubes and engine mounts discussed earlier. The hardest modeling consideration is the rockers. Fortunately ANSYS includes an element known as a revolute joint. This type of joint is found in a door hinge or robot arm, and is a 1-axis joint. While highly configurable, we consider this element only for its ability to model a rigid connection in every direction except about one axis. This represents a rocker very well, as the rocker resists translating in all three directions, and resists rotation in two directions. On the actual Cornell 1999 car the rocker consists of a pivot shaft connected to two tabs. On this pivot shaft are two bearings, one at either end. The rocker pivots on these bearing about the pivot shaft. The bearings are fairly stiff, and any deflection they have is highly nonlinear, so we want to model them as a rigid joint. In ANSYS we set each stiffness value of the rocker joint equal to a very large value (say $1x10^{10}$) to guarantee the joints are not deflecting substantially. This still allows deflection to occur in the tab and rocker shaft, which is what we desire. A table of the different element types as used in the ANSYS model is given below.

ANSYS Element Type	**Use**
Beam4	Round and Square Tubes, gussets, tabs
Link8	Tension/Compression links such as pull links or a-arms
Combin7	Joint for rocker
Combin14	Spring in suspension (can handle damper as well)
Solid45	Solid block used for engine

Using these five elements we can model every load-carrying component of the chassis. The suspension model is only a model, however, and some of the physical geometry has been simplified to make the model easier to construct. For example, the offset between the upright and pull link is a simple stiff beam, which preserves the geometry and load paths, but fails to account for the various actual pieces that are in-between. In addition, no modeling of the wheel, hub or spindle is included. All of these effects mean that the ANSYS model is only an approximation to the real car and will have to be considered when comparing the results to the experimentally determined values.

In addition to modeling the torsional stiffness, this project also considered the dynamic effect of the chassis, such as the frame natural frequencies and vibration modes. In this case the mass21 element was used to distribute

the mass of the car components over the frame. The completed F.E. chassis model is shown below.

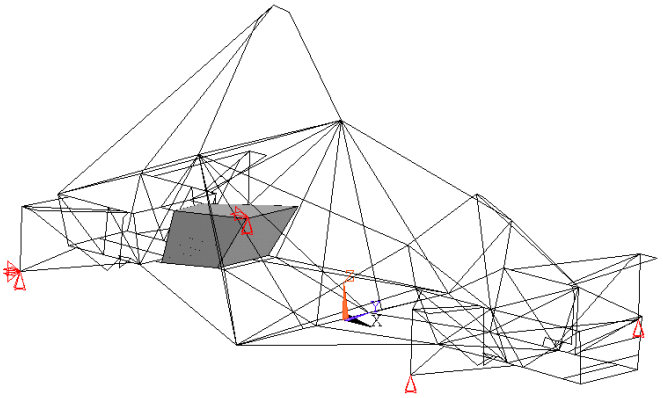

Figure 16: Vehicle Finite Element Model

DYNAMICS

In addition to the static characteristics of the chassis, such as stiffness and strength, there are also dynamic characteristics of interest in handling. One of these dynamic characteristics is the natural frequency. It is important to insure the natural frequencies of the structure are greater than the frequencies of the various load inputs. The simplest calculations we can perform to estimate the natural frequency of a frame or chassis is to assume the frame is a simple tube with two masses at either end. Each of the masses has a moment of inertia, *I*, and the center tube has stiffness, *K*. It is possible to have an applied torque and angular deflection at each end, call them *T* and θ, respectively. If we take the sum of moments about the tube we find

$$\sum T = 0 \Rightarrow I_1 \frac{\partial^2 \theta_1}{\partial t^2} = K(\theta_2 - \theta_1)$$
$$\Rightarrow I_2 \frac{\partial^2 \theta_2}{\partial t^2} = K(\theta_1 - \theta_2)$$

Rearranging we find

$$I_1 \frac{\partial^2 \theta_1}{\partial t^2} = -K\theta_1 + K\theta_2$$
$$I_2 \frac{\partial^2 \theta_2}{\partial t^2} = K\theta_1 - K\theta_2$$

We can represent our variables in matrix form as

$$\{\theta\} = \begin{Bmatrix} \theta_1 \\ \theta_2 \end{Bmatrix}, [I] = \begin{bmatrix} I_1 & 0 \\ 0 & I_2 \end{bmatrix}, [K] = \begin{bmatrix} K_1 & 0 \\ 0 & K_2 \end{bmatrix}$$

Using standard processes for solving an eigenvalue problem yields the characteristic equation as a second order polynomial given by

$$\lambda^2 + \left(\frac{K}{I_1} + \frac{K}{I_2}\right)\lambda + \frac{K}{I_1 I_2} = 0$$

The solution of the characteristic equation gives

$$\theta_1 = v \cdot \cos(\omega_n t)$$
$$\theta_2 = v \cdot \sin(\omega_n t),$$

And the natural frequency is given by

$$\omega_n = \sqrt{-\lambda}$$

To study a representative case consider a frame with stiffness 1500 ft-lbs/degree (366 kN m/rad) and two masses with inertia 7 kg m^2. We find our natural frequency is 230 rads/sec or 36 Hz. The rotating wheels of the car cyclically load the frame and we wish to know at what speed we reach the natural frequency. Knowing the tire radius we can calculate the speed to reach the natural frequency, 130 mph in this case. This gives a safety factor of two, since maximum speed is usually constrained to be below about 65 mph in FSAE events due to track layout.

The above example shows some of the steps for solving the very simple problem presented. We can imagine that as we split the domain into a series of springs and masses we get a better result. Taking very small pieces we begin to reach a finite element analysis, which is the subject of the next section.

The natural frequencies and mode shapes can be calculated for the overall chassis by adding elements representing the distributed mass present in the vehicle. To begin with, we assume the mass of the car is uniformly distributed throughout the frame tubes. Performing a modal analysis we find the following natural frequencies.

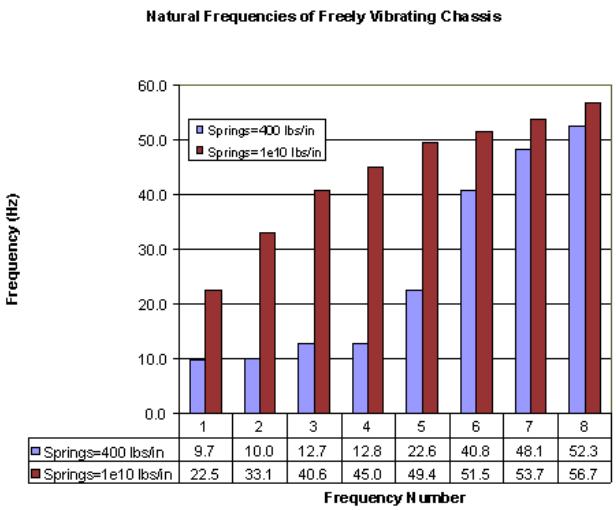

Figure 17: Chassis Natural Frequencies

The mode shapes corresponding to the frequencies are shown below:

Mode #	Freq. (Hz)	Mode Shape
1	9.7	Pure torsion between the front and rear of the car
2	10.0	Rear Suspension "Flapping" - Vertical motion at king pins with relatively fixed position at frame
3	12.7	Torsional mod with Suspension/Frame out of phase
4	12.8	Front Suspension "Flapping"

The “flapping” mode takes it name because it resembles a bird in flight. A picture of the 10.0 Hz “flapping” mode is shown below for the rear suspension

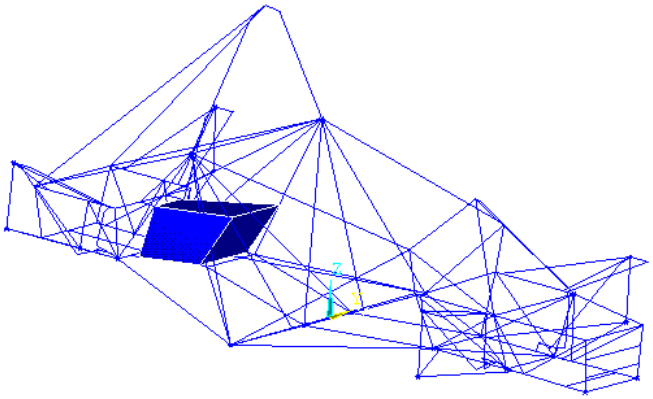

Figure 18: Chassis Free Vibrating Mode 2

A better mass distribution approximation is to represent each component of the car with one or more mass elements positioned correctly in car space. Larger masses, such as the driver, were split into discreet point masses and connected by rigid links to their mounting points, such as the seat and seat belt mounts in the case of the driver. The masses and positions were tweaked until the center of gravity matched what was measured in the lab. Interestingly, making a detailed model and rerunning the modal analysis yielded very similar results to the simple uniformly distributed mass assumption for the global modes. The suspension mode shifted when the springs were not rigid because of the better approximation of the unsprung weight but remained mostly unchanged when the springs were rigidly modeled.

EXPERIMENTS

FRAME TORSION TEST

Once the frame is built it is important to verify the math models and determine exactly what characteristics the structure has achieved. A simple methodology and analysis technique is presented below to determine frame torsional stiffness.

Torsional loads, induced by an undulating road surface or cornering forces are one of the most important and highest magnitude loads transmitted through the frame. To analyze the torsional rigidity of a car frame, a simple model can be to assume one end of the car is fixed, and the frame is a hollow tube, with a moment applied at one end. This is shown schematically.

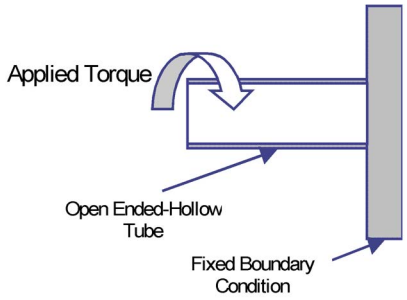

Figure 19: Torsion Tube

This concept, when applied to the real car frame would look like follows

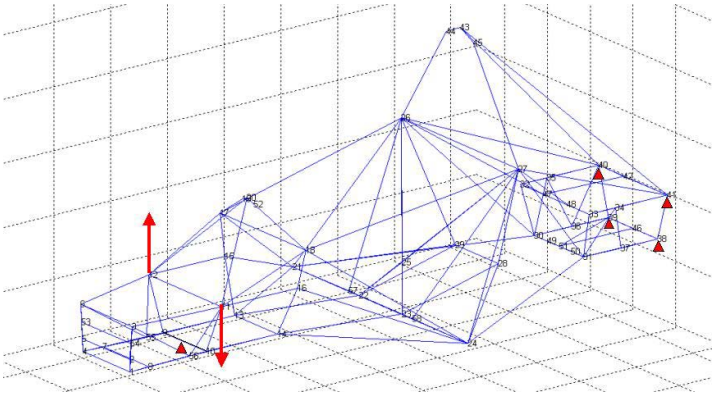

Figure 20: Frame Finite Element Model Loading Case

The torsional rigidity can be calculated by finding the torque applied to the frame (the tube) and dividing by the angular deflection. The actual calculation is done as follows, with the picture below showing a view looking from the front of the suspension bay.

$$K = T/\theta$$

$$K = \frac{FL}{\tan^{-1}\left[\left(\Delta y_1 + \Delta y_2\right)/2L\right]}$$

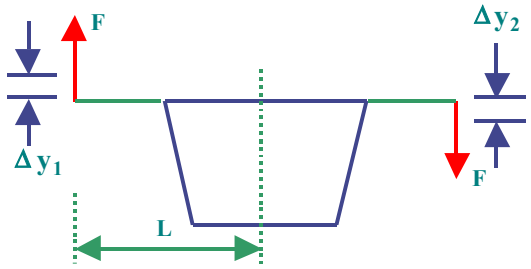

Figure 21: Front Suspension Bay Testing Loads

The torque defined above is the product of the force applied at one corner, and the distance from the point of application to the centerline of the car. The deflection is taken to be angle formed from the center of the car to the position of the deflected corner. The reason both deflections occur in the above equation is we take the average of the left and right deflections to generate a more accurate estimate of the total angular deflection. The above example is rather difficult to produce in the lab, because of the need to generate a vertical force counter to the direction of gravity. It would be much simpler to just hang a known weight on one corner of the car and allow it to pivot about a roller. This method is shown below.

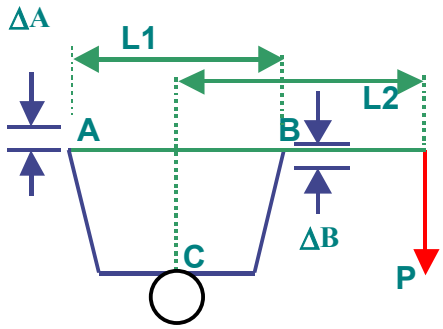

Figure 22: Front Suspension Bay Testing Loads

In the above figure note that the lever arm is a tube clamped to the frame at points A and B. A weight is then hung from the end of the tube. The frame is supported on its centerline by a roller at point c. The torque acting on the car and resisted at the clamped rearbay is simply the force, P, times the lever arm, L2. The angle of twist can be simply calculated from the average deflection and the half bay width or

$$\theta = \tan^{-1}\left(\frac{\Delta_A + \Delta_B}{L_1}\right)$$

Now we only have to use the definition of torsional stiffness, and substitute in our expressions for the torque and angular deflection.

$$K = \frac{T}{\theta}$$

$$K = \frac{P(L_1 + 2L_2)}{\tan^{-1}\left(\frac{\Delta_A + \Delta_B}{L_1}\right)}$$

This method of frame testing is relatively straightforward and the advantage is the frame stiffness can be determined without including the suspension components. The primary disadvantage is the artificially created load paths do not load the frame in the same manner as on the track. Also, the choice of what rear nodes to fix, and what front nodes to apply the load can affect the results significantly. For this reason a whole car chassis torsion test is the preferred method for capturing the true vehicle stiffness.

FULL CHASSIS TORSION TEST

A better way to assess the structures capabilities is to twist test the entire chassis assembly. There are a variety of methods to load a chassis in torsion. One of these methods is discussed in [1]. This method involves constructing a fixture with two jacks at the front of the car, and two fixed supports at the rear. The two front jacks are moved through an equal and opposite displacement. Each of the four supports is equipped with a load cell to output the force at each corner. One advantages of this method is the car is put in pure torsion, because the pivot point of the displacement is aligned with the front end of the car. Additionally, the supports provide near minimal-constraint that produces a more accurate answer. While this method would be quite nice, it involves constructing a test fixture, and this fixture needs to then be secured to the ground.

Another method, and the method actually used to acquire the data, uses the suspension corner weight scales and camber plates. A picture of the testing setup is shown below

Figure 23: Testing Setup for Front Left Corner

The camber plates are large aluminum plates that are bolted to the hubs and usually used to set the camber accurately. The corner weight scales are four load cell scales that measure the weight on each corner of the car. To conduct the test, first place all four camber plates on the car. Next, configure the scales. The scales should be placed so the car can later be placed on top of them. A scissors jack is used to apply a deflection at one corner of the car. Place the scissors jack at one of the front corners (the driver's left was used for these tests) and spacers of the same height as the fully retracted jack at the other three corners. With these in place locate the car on the spacer/scale assemblies. The next step is to locate dial indicators at all positions to be tested. An indicator was located at the point of application of the load – i.e. where the scissors jack lifted the camber plate. The dial indicator was then positioned to read off a suitable position of the upright/hub. The distance between the front camber plates was measured to calculate the torsional stiffness.

With the car securely located on the scales, and the jack ready, stiffness can be tested. Frame testing over the years has revealed very linear results for twist tests. The frame is primarily a welded steel structure. Chassis testing, however, has very high non-linearity in the early stages. For small forces gaps in the suspension and compression of various bearing elements occurs. As these gaps are closed and bearing friction is overcome the slope of the load deflection curve becomes linear. For this reason, it is necessary to map the force-displacement characteristic of the structure, rather than finding one stiffness value. To get better data small steps of load should be applied, and the corresponding displacement measured. It is also interesting to note that the force deflection curve has some hysteresis. To accurately gauge this characteristic, it is helpful to add or remove the load in finite steps and record the deflection. This will build a load deflection "path" that rises and then falls again. . At high loads the deflection is linear. This represents the deformation of the elastic frame and suspension members after gaps are closed. A sample graph is shown below.

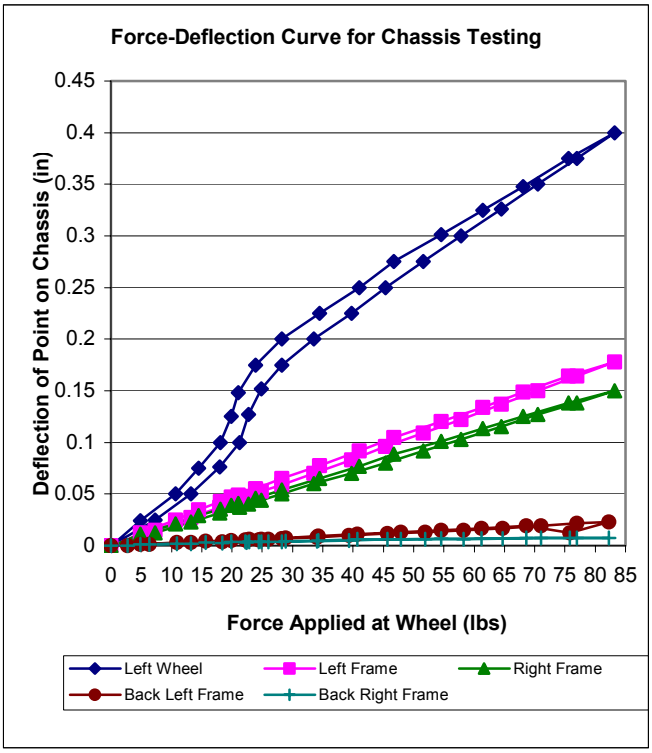

Figure 24: Twist Test Force-Deflection Curve

If we take a compilation of these graphs and present only the linear region the results would look like the following:

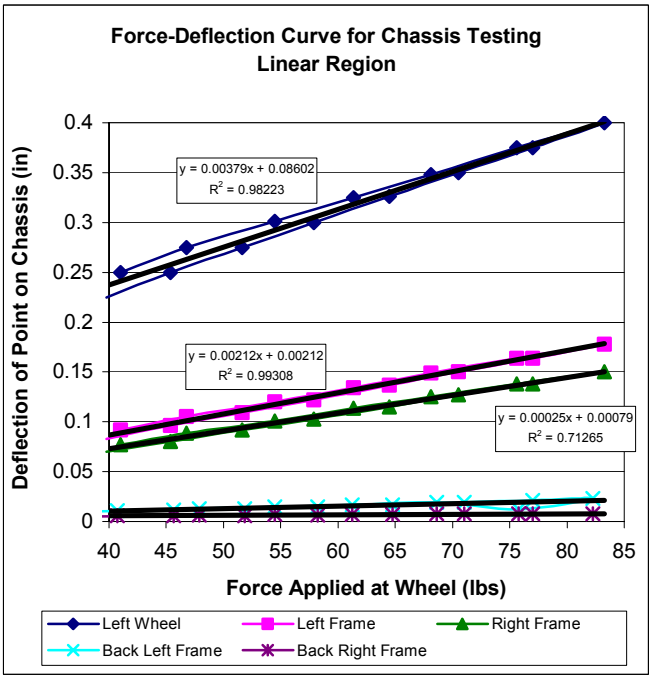

Figure 25: Twist Test Force-Deflection Curve Linear Region

Note in the above chart the force is applied through a jack at the left wheel. All other wheels are fixed to ground. It is clear from the chart that the point on the chassis where the load is applied deflects the most. As we move away from this point the deflections decrease, as expected. To compare the relative motion of the

different points we can tabulate the values for all the deflections at a point where the wheel has moved vertically 0.100". Using the ANSYS chassis model that was developed in section 8 of this paper, and applying a 0.100" deflection to the wheel, we are able to determine the resulting deflection of the other points as well as the force necessary to achieve these displacements.

A comparison of the ANSYS results and experimental results is given below:

	Applied Displ.	**Frame Front**		**Frame Back**	
	Front Left Wheel	Left	Right	Left	Right
ANSYS	0.100	0.058	0.044	0.011	0.002
Experiment	0.100	0.054	0.046	0.007	0.001
Difference		7%	-3%	47%	51%

Note that the experimental values were normalized to a wheel deflection of 0.100" for ease of comparison. The agreement between these two data sets is fairly high. We see the largest difference is 0.004" while the smallest is 0.001". The variation in values is primarily due to the simplified suspension model and discrepancies in the ratio of the front and rear suspension stiffness. This will be discussed in more detail shortly. The large percentage errors at the rear of the frame are due to the very small magnitude of the measurements.

The above tests were all conducted with solid elements in place of the shock absorbers. In the experiment these consisted of aluminum tubes with rod ends in either end and with the same length as the shock/spring at ride height. In the ANSYS model the stiffnesses of the spring elements was set to $1x10^6$ pounds/in.

Using the experimental data we can now calculate the stiffness of the chassis. The chassis stiffness in this case will be the torsional stiffness, expressed in foot-lbs per degree, of the frame and suspension. Note that this value will be calculated with very stiff suspension springs. To calculate the chassis stiffness we need to know the front track and the force and deflection of the front wheel. The following table shows the pertinent values for our standard ANSYS model as well as the experimental results:

	ΔF	Δd	Track	Torque	Angle	Stiffness
	lbs	in	in	ft-lbs	deg	ft-lbs/deg
Experiment	43.5	0.175	44	159.5	0.228	700
ANSYS Model	100	0.262	44	366.7	0.342	1073

The equations used to calculate the values in the chart are as follows:

$$Torque = T = \Delta F \cdot Wheelbase = \frac{\Delta F \cdot Wheelbase}{12} = \frac{[lbs]\cdot[in]}{[in/ft]} = [ft]\cdot[lbs]$$

$$Angle = \theta = \tan^{-1}\left(\frac{\Delta d}{Wheelbase}\right) = [\text{deg}]$$

$$Stiffness = K = Torque / Angle = T/\theta = \frac{[ft\cdot lb]}{[\text{deg}]}$$

If a regression line is fitted to the Force-Deflection curve a chassis stiffness value of 743 ft-lbs/deg is found. The calculation differs by using the slope of the wheel force-deflection curve as the chassis stiffness in pounds/inch. This is then converted to a torsional value using the track similarly to the above equations. Note that this gives an average value for bump and rebound as the curve is fitted between the high and low values of the force-deflection path.

The difference between the experimental and mathematical data, using 743 ft-lbs/deg as our experimental value, is 330 ft-lbs/degree or roughly 30%. To understand where this error comes from we must look at both the experimental setup and the mathematical ANSYS model.

The experimental error can arise from several key areas:

1. Inaccuracy of the load cells within the chassis setup scales used to measure the reaction loads
2. Gradual drift in the load cells
3. Inaccuracy of the dial indicators used to measure deflection
4. Slipping of the dial indicator on its pickup point
5. Binding in the suspension, especially the camber plates on the blocks

To test for drift in the load cells a fixed weight was placed on the scales and the corresponding reading was measured over fixed intervals. It was found that the reading held constant for several hours, much longer than the time needed to record a force as the chassis was twisted. To test for slipping the dial indicators were observed throughout the test to confirm they were solidly mounted. Friction between the camber plates and blocks was unavoidable in the present configuration. Perhaps future tests could be conducted using the low-friction supports used to test the steering system for driver effort. The remaining two error sources, specifically error in either the scales or indicator can be estimated using the following procedure. Note we are not considering the track measurement. An error in the track measurement of even 1/8" makes only a 4 ft-lb/deg difference in chassis stiffness.

To estimate the error we independently estimate the error arising from the force measurement and the displacement measurement. If we assume a Gaussian distribution of error we can calculate the cumulative error by the following equation:

$$\delta_y = \sqrt{\sum_{i=1}^{N} \left(\frac{\partial F}{\partial x}\right)^2 \delta_i^2}$$

Here we are calculating the cumulative error by using a root-mean-square addition of the error terms from each aspect of the equation. Our Equation for chassis stiffness, combining terms from the derivation earlier in this section is as follows:

$$K_{chassis} = \frac{T}{\theta} = \frac{F_{wheel} \cdot L}{\tan^{-1}\left(\frac{\Delta}{L}\right)} = \frac{\left(\frac{44}{12}\right) \cdot F_{wheel}}{\tan^{-1}\left(\frac{\Delta}{44}\right)}$$

calculating the tangent in degrees. Since we have to take derivatives it becomes very convenient to make the small angle approximation to the preceding equation. In this case the chassis stiffness is given by

$$K_{chassis} = \frac{F_{wheel} \cdot \left(\frac{L}{12}\right)}{\tan^{-1}\left(\frac{\Delta}{44}\right)} = \frac{F_{wheel} \cdot \left(\frac{L}{12}\right)}{\frac{180}{\pi}\left(\frac{\Delta}{L}\right)} = \frac{\pi \cdot F_{wheel} \cdot L^2}{2160 \cdot \Delta}$$

where L, the track, is measured in inches. The additional term in the denominator arises from converting from radians to degrees. We now take partial derivatives of stiffness with respect to the variables of F and Δ.

$$\frac{\partial K}{\partial F} = \frac{\pi \cdot L^2}{2160 \cdot \Delta}$$
$$\frac{\partial K}{\partial x} = -\frac{\pi \cdot F \cdot L^2}{2160 \cdot \Delta^2}$$

If we assume the error in our measurements as follows

$$\delta F = \pm 1$$
$$\delta \Delta = \pm 0.001$$

then writing out the individual terms for the summation given above we find our error can be calculated directly from the following equation

$$\delta K = \sqrt{\left(\frac{\pi \cdot L^2}{2160 \cdot \Delta}\right)^2 \cdot \delta F^2 + \left(-\frac{\pi \cdot F \cdot L^2}{2160 \cdot \Delta^2}\right)^2 \cdot \delta \Delta^2} = 27.9\, ft \cdot lbs / \deg$$

Our error is shown above as 27.9 ft-lbs/deg or roughly 4% of 700 ft-lbs/deg, the measured value. Analyzing the numerical values of the error for each variable shows the results are much more sensitive to errors in the scale reading than in the dial indicator measurement. This makes intuitive sense since a few thousandths out of a quarter inch of travel is very small compared to even one pound compared to a force of 50 lbs. Using even conservative estimates for our errors shows the chassis stiffness values we are calculating are a reliable estimation of the actual stiffness.

Looking next at the analytic model of the chassis, the total error can be attributed to the individual errors in the frame and suspension components. Since the frame model was verified by twist-testing the frame alone, the frame model should be accurate. The suspension model, however, is a simplified model and should be more stiff than the actual suspension. Hand calculations on the links inserted to replace the spring/damper in the experiments shows that their stiffness is close to the modeled value of 1.0×10^6 pounds/in. Therefore the error must be due primarily to the other elements of the suspension, such as uprights, a-arms, gussets, tabs, rod ends, and, of course, the hub and spindle assemblies which are not modeled at all.

The overall suspension stiffness can be modeled a variety of ways. Each of the individual components could be modeled to calculate its actual stiffness, which should then predict the reduced stiffness that was measured in the lab. However, given the limited experimental data consisting of the deflections of the wheel and four points on the frame, the best approach seemed to be modifying the overall suspension stiffness until the model matched the experimental results. To achieve this the suspension was assigned its own material property. Initially the Young's Modulus of this material is set to that of steel, or 30×10^6 psi, but is gradually changed until the chassis stiffness matches that measured by the twist tests. An equivalent suspension Young's Modulus of 12×10^6 psi, found by iteration yielded a good match, producing a chassis stiffness of 740 ft-lbs/deg.

One other way to gauge in discrepancies between the model and experiment is to measure twist along the length of the frame. This will pinpoint the regions of the structure where the deflections are different or similar to the predicted values. An example of a plot showing the deflections along the length, plotted by position is shown below. The graph is made from the ANSYS results. This type of chart can be made with either vertical deflection or angular twist. The angular twist is a better measure because when vertical deflection is plotted, nodes that are farther from the center of twist will deflect more vertically and appear as much larger values. Angular deflection eliminates distance from the twist axis as a variable.

In the chart below, notice how the graph is aligned to match the plotted points to their corresponding node on the frame graphic. Two lines are shown representing the top and bottom of the car. The top and bottom nodes will deflect different amounts due to the geometry of the frame and forces acting to either push apart or pull together the structure. The term bay spread is given to this pushing/pulling force and deflection and has to be taken into account to accurately gauge the structural stiffness from the experiments.

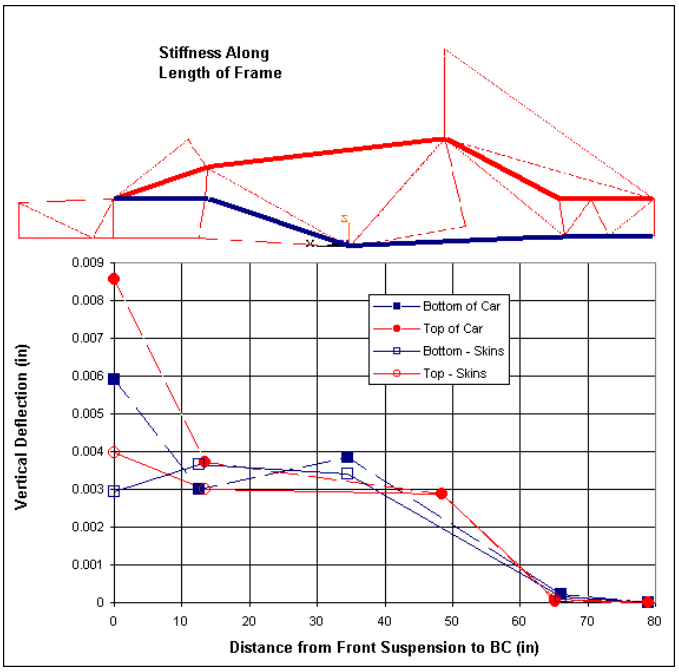

Figure 26: Deflection Along Vehicle Length

The slopes of the lines in different regions of the chart show the relative effectiveness of each section of the frame. Regions of high slope show where the majority of the compliance is occurring. Data is included prior to and after the bonding and attaching of the stressed aluminum skins. As expected, the front and rear bays of the car show a marked improvement in torsional stiffness after bonding of the skins, while the cockpit region shows a relatively fixed stiffness. This is because the front bay in particular is designed to be fully triangulated only with the skins in place, while the cockpit region is a fully triangulated structure independent of the stressed skins. The cockpit region also has a relatively large cross sectional area compared to the other parts of the car.

CONSIDERATION OF CHASSIS STIFFNESS FOR OPTIMAL SUSPENSION OPERATION

The most accurate way to determine proper chassis stiffness is through testing and experience. Teams that have competed over several years gain experience about which cars were tunable and what levels of chassis stiffness were appropriate. Since the suspension is designed around the assumption that the frame and suspension components are rigid they need to have stiffness values several times greater than the compliant suspension members. One general rule of thumb found in literature is a structural stiffness ten times (one order of magnitude) greater than the spring rates. Opinion differs, however, and some will express a stiffness target in terms of a multiple of spring rate, tire rate, wheel rate or a certain frequency. In the one wheel bump model discussed in this paper it is usually feasible to build a reasonable structure that has 90% of the stiffness of theoretical rigid chassis. Higher values can be obtained with further optimization or a weight penalty.

Given a 400 lb/in spring and including the tire, the 1999 car frame and suspension stiffness is highly efficient (91% of the rigid case). Currently lower spring rates are used which for the same structure gives an even greater efficiency. A 200 lb/in spring increases the efficiency to 94%.

Cornell frames have varied in stiffness from 1000 ft-lbs/deg to 2000 ft-lbs/deg over the last decade. The table below presents some data. The values are those quoted historically and do not represent a retest of old cars. Variability between the tests is certain and could be a large fraction of the total value. For that reason values should be taken as only indicative of the actual values.

Year	Stiffness ft-lbs/deg	Weight lbs	K / W ft-lbs/deg/lb
1999	1600	57	28.1
1998	1600	57	28.1
1997	1600	58	27.6
1996	1400	60	23.3
1995	1000	60	16.7
1993	2000	50	40.0

Clearly, the 1993 car had an extremely efficient chassis, and was an all around good performer with a first place finish. It made use of the Honda CBR engine where the other cars all employed the Yamaha FZR. The Honda engine had different engine mounts that allowed for a more fully stressed engine and reduced the weight of the frame significantly. In addition to the '93 car the '97, '98 and '99 cars were all regarded as having good dynamic performance and responded to tuning changes.

The historical data shows that Cornell frames have recently clustered around 1600 ft-lbs/deg. Based on the mathematical and antidotal data we can put the following picture together:

1. Drivers of past cars which were below 1600 ft-lbs/deg stiffness often complained of flexibility and a lack of suspension control – though it is difficult to isolate this purely to lack of frame stiffness.
2. Weight savings for the earlier lower stiffness cars compared to recent cars is not as significant as might be imagined.

Just as important as the frame, and perhaps more important, is the stiffness of the suspension links and components. They factor in to the hub-to-hub torsional stiffness but their compliance can drastically alter the predicted kinematic motion of the tire. In order to maintain the targeted camber, castor and toe behavior the suspension links compliance has to be small in magnitude relative to the kinematic component of the motion. Trading off stiffness to weight is ultimately the key to a successful racecar, but the recommendation that arises from all this data taken together is that the

present value for frame stiffness of roughly 1600 ft-lbs/degree is a good compromise of stiffness, weight and safety when coupled with a suspension structural stiffness that is approximately equal. This achieves efficiency relative to a rigid structure of around 90% in one wheel bump.

CONCLUSION

This paper has considered a variety of issues related to frame and chassis design with an emphasis on Formula SAE cars. The different road loads and deformation modes were considered as well as some generic design targets based on experience and strain gauged suspension links. A simple mathematical model was developed for comparing the structural stiffness to the suspension stiffness to gain insight into proper design targets for the vehicle structure. These charts also aid in visualizing the tradeoff between stiffness and weight the designer must make. With these stiffness targets in mind, a finite element model was constructed for both the frame in isolation as well as the entire chassis/suspension. This model was constructed and analyzed in ANSYS. Finally, some experimental methods were presented with an emphasis on the whole-car torsion procedure. This method best captures load paths, suspension contributions and is easily performed by teams as they prepare for the competition.

ACKNOWLEDGMENTS

This work is based to a great extent on the experience and corporate memory of sixteen years of Formula SAE participation by the Cornell University teams. Without the efforts of many previous team members, mentors and advisors this paper would not have been possible.

REFERENCES

1. Thompson, L.L, Law, E. Harry and Lampert, Jon, “Design of a Twist Test Fixture to Measure Torsional the Torsional Stiffness of a Winston Cup Chassis”, SAE Paper 983054
2. Costin, Michael and Phipps, David, “Racing and Sports Car Chassis Design”, B.T. Batsford Ltd., 1961
3. Milliken, William F. and Milliken, Douglas L., “Race Car Vehicle Dynamics”, Society of Automotive Engineers, 1997
4. Foale, Tony, “Motorcycle Chassis Design: Theory and Practice”, Osprey Books, 1984
5. Fenton, John, “Vehicle Body Layout and Analysis”, Mechanical Engineering Publications, 1980
6. Fenton, John, “Handbook of Vehicle Design Analysis”, Society of Automotive Engineers, 1996
7. Heisler, Heinz, “Vehicle and Engine Technology”, Society of Automotive Engineers, 1998
8. Heisler, Heinz, “Advanced Vehicle Technology”, Edward Arnold, 1989
9. Mitschke, M., “Dynamik Der Kraftfahrzeuge: Band A: Antrieb Und Bremsung”, 1996
10. Young, Warren C., “Roark’s Formulas for Stress and Strain”, McGraw Hill, 1989
11. Fraser, Donald, “Conceptual Design and Preliminary Analysis of Structures”, Pitman Publishers Ltd., 1981
12. Cox, H. L., “The Design of Structures of Least Weight”, Pergamon Press, 1965
13. McGuire, William, Gallagher, Richard H., et al, “Matrix Structural Analysis, 2nd Edition”, John Wiley & Sons, 1999
14. Cook, Robert, “Finite Element Modeling for Stress Analysis”, John Wiley & Sons, 1995
15. Cook, Robert, Malkus, David S. and Plesha, Michael E., “Concepts and Applications of Finite Element Analysis”, John Wiley & Sons, 1989
16. Kwon, Young W., Bang, Hyochoong and Kulacki, Frank, “The Finite Element Method Using Matlab”, CRC Publishers, 1996
17. ANSYS Online Documentation
18. Megson, T.H.G. and Megson, T.U.G, “Aircraft Structures for Engineering Students”, Halsted, 1999
19. Donaldson, Bruce, “Analysis of Aircraft Structures: An Introduction”, McGraw Hill College Division, 1992
20. Bruhn, E.F., “Analysis and Design of Flight Vehicle Structures”, Jacobs Publishing, 1973
21. Peery, David J., “Aircraft Structures”, McGraw Hill College Division, 1982
22. Chun-Yung, Michael and Niu, Mike, “Airframes Structural Design: Practical Design Information and Data on Aircraft Structures”, Technical Book Co., 1999